

Article

Second-Order Sidebands and Group Delays in Coupled Optomechanical Cavity System with a Cubic Nonlinear Harmonic Oscillator

Qiwen Zhao ¹, Ying He ^{1,*} , Yanfang Yang ¹, Huifang Zhang ¹ and Yi Xu ² ¹ Department of Physics, College of Science, Shanghai University, Shangda Road 99, Shanghai 200444, China² School of Optoelectronic Engineering, Guilin University of Electronic Technology, Guilin 541004, China

* Correspondence: heying@shu.edu.cn

Abstract: The generation of second-order sidebands and its associated group delay is an important subject in optical storage and switch. In this work, the efficiency of second-order sideband generation in a coupled optomechanical cavity system with a cubic nonlinear harmonic oscillator is theoretically investigated. It is found that the efficiency of second-order sideband generation can be effectively enhanced with the decrease in decay rate of optomechanical cavity, the increase in coupling strength between two cavities and the power of probe field. The slow light effect (i.e., positive group delay) is also observed in the proposed optomechanical cavity system, and can be controlled with the power of control field.

Keywords: optomechanical cavity; cubic nonlinear harmonic oscillator; second-order sidebands; group delay



Citation: Zhao, Q.; He, Y.; Yang, Y.; Zhang, H.; Xu, Y. Second-Order Sidebands and Group Delays in Coupled Optomechanical Cavity System with a Cubic Nonlinear Harmonic Oscillator. *Photonics* **2024**, *11*, 256. <https://doi.org/10.3390/photonics11030256>

Received: 18 January 2024

Revised: 8 March 2024

Accepted: 11 March 2024

Published: 12 March 2024



Copyright: © 2024 by the authors. Licensee MDPI, Basel, Switzerland. This article is an open access article distributed under the terms and conditions of the Creative Commons Attribution (CC BY) license (<https://creativecommons.org/licenses/by/4.0/>).

1. Introduction

Cavity optomechanics is an important field that combines optics and mechanics. It focuses on the interaction between the light in a resonant cavity and the cavity mirror for mechanical vibration through the radiation pressure of light [1]. This interaction can be used on macroscopic gravitational wave detectors or microscopic scanning electron microscopy cantilevers. Due to its important research value in quantum communication and quantum computing [2] and ultrasensitive force measurement [3], cavity optomechanics has received considerable attention. Recent experiments have proved the possibility of cooling the mechanical oscillator to the quantum ground state in a cavity optomechanical system [4,5], which enables us to explore many nonlinear optical phenomena in optomechanical systems [6–8], such as the non-classical correlations between phonons and single photons [9], entanglement between mechanical and optical resonators [10,11], parametric normal-mode splitting [12–14], and mechanical compression state below zero point fluctuation [15–17]. In addition, electromagnetic induced transparency (EIT) effect has been widely discussed in quantum optics. It refers to the phenomenon that a medium composed of three-level or multi-level atoms becomes transparent to weak detection fields under the action of a strong driving electromagnetic field [18–21]. EIT has potential applications in enhancing nonlinearity [22], realizing fast light and slow light [23], quantum storage [24], and light switching [25]. The optomechanically induced transparency (OMIT), an analogue of EIT, can be reached in cavity optomechanical systems [19,26,27]. The basic mechanism of OMIT is the dissipative interference between the detection field photons and the upconversion sideband photons generated by the anti-Stokes process in the cavity optomechanical system, thus resulting in an adjustable transparent window of the detection light in the resonance region that should have been strongly absorbed.

The slow light effect based on OMIT has attracted considerable attention in recent years [20,28–32], which resulted in the anomalous dispersion of the system at the transparent window. OMIT has become a very important path for delaying, slowing down,

and storing light signals. The second-order or higher-order sidebands can be generated in the cavity optomechanical system through the quantum operation of OMIT [33–35]. The generation of second-order sidebands [35] is a classic optical nonlinear phenomenon. When the control field and detection field are incident on an optomechanical system, the optomechanical interaction generates photons at the second-order sidebands. It has been demonstrated that the generation of the second-order sideband can improve the accuracy in charge and micro mass measurements [36–38].

However, most studies on the OMIT and second-order sidebands in cavity optomechanical systems are conducted with linear mechanical oscillators [19,27,33,37,39]. The neglect of the nonlinearity of mechanical oscillators can be attributed to its inherent weak nonlinearity. The cubic nonlinearity and Duffing quartic nonlinearity (i.e., fourth-order nonlinearity) are two typical nonlinearities of mechanical oscillators [40–42]. In recent years, it has been demonstrated that the weak nonlinear strength of mechanical oscillators can be significantly enhanced, for example, by engineering the material and geometrical effects of mechanical oscillators [43], introducing the electrostatic actuation [43], coupling with a low-dimensional auxiliary system [44], and using the chemical bonding force [42]. The enhanced nonlinearity of mechanical oscillators provides the opportunity to study various interesting phenomena in cavity optomechanical systems with nonlinear mechanical oscillators [6,41,45–49]. For example, Lü et al. found that strong steady-state mechanical squeezing can be achieved in a cavity optomechanical system with the Duffing nonlinearity or cubic nonlinearity [41]. The normal mode splitting [47], OMIT [6,48], and the stationary optomechanical entanglement [50] in a cavity optomechanical system with a cubic nonlinear movable mirror were also investigated in recent years. It was found that the introduction of cubic nonlinearity in the cavity optomechanical system results in an asymmetric line shape of the OMIT window [6]. The cubic or quartic nonlinearity of a mechanical oscillator in a cavity optomechanical system can be precisely measured by monitoring the phase shift of the optical field interacted with the anharmonic oscillator [51].

In a conventional cavity optomechanical system, the mechanical oscillator is usually treated as a harmonic oscillator and has a quadratic potential, which is a quadratic function of the position. Here, in this work, the cubic nonlinearity of a mechanical oscillator is considered in the cavity optomechanical system. In this case, in addition to the quadratic potential term, this mechanical oscillator has a cubic potential term. This work studied the generation of second-order sidebands in a coupled optomechanical cavity system with a cubic nonlinear harmonic oscillator. The effect of the mechanical nonlinearity strength, the cavity decay rate, the coupling strength between two cavities, and the power of the control and probe field on the efficiency of the second-order upper sideband are investigated. In addition, the group delay of the second-order sidebands is also discussed.

The remainder of this paper is structured as follows. In Section 2, we describe the proposed coupled optomechanical cavity system with a cubic nonlinear harmonic oscillator, and give the expressions of the steady-state solutions and coefficient of the second-order upper sideband in the proposed coupled optomechanical cavity system. The effects of various parameters (e.g., mechanical nonlinearity strength and cavity decay rate) on the efficiency of the second-order upper sideband are discussed in Section 3. Finally, the results are summarized in Section 4.

2. Theoretical Model

The schematic diagram of the proposed coupled optomechanical cavity system with a cubic nonlinear harmonic oscillator is shown in Figure 1. The optomechanical cavity system studied in this work consists of an optical cavity a with a mechanical oscillator and an optical cavity b . The frequencies of the two cavities a and b are ω_a and ω_b , respectively. The decay rate of cavity a is κ_a , and κ_b is the decay rate of optical cavity b . The two cavities a and b are coupled to each other with the coupling strength J . The left side of the cavity a is a fixed mirror which is partially transparent. The right side of the cavity a is a movable mirror which is fully reflective, and the right mirror is a cubic nonlinear mechanical oscillator.

The nonlinear mechanical oscillator has the effective mass m and resonant frequency ω_m . A strong control field with frequency ω_c and amplitude ε_c , and a weak probe field with frequency ω_p and amplitude ε_p are projected into the optical cavity a through the fixed mirror on the left side. The strong control field is adopted to drive the coupling between the cavity field and the mechanical oscillator, while the weak probe field is used to detect the system response.

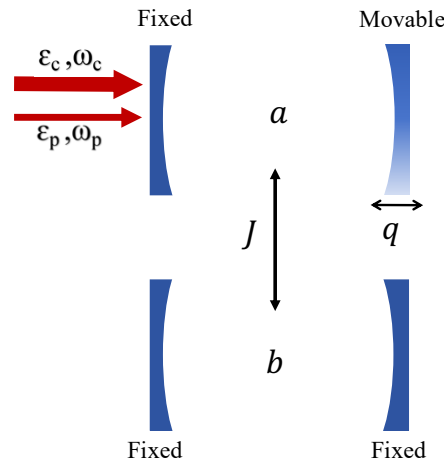


Figure 1. Schematic diagram of the proposed coupled optomechanical cavity system with a cubic nonlinear harmonic oscillator.

The Hamiltonian of the proposed cavity optomechanical system is given by

$$H = \hbar\omega_a \hat{a}^\dagger \hat{a} + \hbar\omega_b \hat{b}^\dagger \hat{b} + \hbar J (\hat{a}^\dagger \hat{b} + \hat{b}^\dagger \hat{a}) + \hbar g \hat{a}^\dagger \hat{a} \hat{q} + \frac{\hat{p}^2}{2m} + \frac{1}{2} m \omega_m^2 \hat{q}^2 + \frac{1}{3} \alpha \hat{q}^3 + i\hbar\varepsilon_c (\hat{a}^\dagger e^{-i\omega_c t} - \hat{a} e^{i\omega_c t}) + i\hbar\varepsilon_p (\hat{a}^\dagger e^{-i\omega_p t} - \hat{a} e^{i\omega_p t}), \tag{1}$$

where \hat{a} and \hat{a}^\dagger (\hat{b} and \hat{b}^\dagger) represent the annihilation operator and creation operator of the cavity a (cavity b), respectively. g denotes the optomechanical coupling constant. \hat{q} and \hat{p} describe the displacement operator and momentum operator of the mechanical oscillator with a damping rate γ_m , which has the relationship of $[\hat{q}, \hat{p}] = i\hbar$. The amplitudes of the control field and the probe field are $\varepsilon_c = \sqrt{2\kappa_a \wp_c / \hbar\omega_c}$ and $\varepsilon_p = \sqrt{2\kappa_a \wp_p / \hbar\omega_p}$, respectively. Here, \wp_c is the power of the control field, and \wp_p is the power of the probe field.

The first and second terms of the Hamiltonian in Equation (1) describes the cavity photon modes in cavity a and b , respectively. The third (fourth) term indicates the coupling between the photon mode in cavity a and photon mode in cavity b (mechanical mode) with the coupling strength J (g). The term $\hat{p}^2 / (2m) + m\omega_m^2 \hat{q}^2 / 2 + \alpha \hat{q}^3 / 3$ describes the Hamiltonian of the movable mirror, which can be regarded as a harmonic oscillator with a cubic term (i.e., $\alpha \hat{q}^3 / 3$) perturbation [52]. The parameter α is the mechanical nonlinearity strength of the mechanical oscillator, and different values of α will lead to different coupling-constant behavior [53]. The terms $\frac{\hat{p}^2}{2m} + \frac{1}{2} m \omega_m^2 \hat{q}^2 + \frac{1}{3} \alpha \hat{q}^3$ denote the kinetic energy and potential energy of the simple harmonic oscillator. In contrast, the nonlinear term $\alpha \hat{q}^3 / 3$ is directly proportional to the third-order of the displacement q , which describes the potential energy produced by the nonlinearity of the cubic nonlinear harmonic oscillator. It is assumed that the quadratic potential energy $m\omega_m^2 \hat{q}^2 / 2$ is much larger than the cubic potential energy $\alpha \hat{q}^3 / 3$, and thus the cubic potential energy $\alpha \hat{q}^3 / 3$ can be considered as a perturbation. The cubic nonlinear simple harmonic oscillator is a most classical example of perturbation in harmonic oscillator in quantum mechanics. Various studies on the cubic nonlinear simple harmonic oscillator have been reported in recent years, such as the resonance eigenvalue [54] and periodic motion [53] of the cubic nonlinear simple harmonic

oscillator with a real mechanical nonlinearity strength, the ground state energy [55,56] and the Stark effect [57] of the cubic nonlinear simple harmonic oscillator with a complex mechanical nonlinearity strength. Here, the mechanical nonlinearity strength α is assumed to be positive and real for simplicity in this work.

The Hamiltonian in Equation (1) can be rewritten as

$$H = \hbar\Delta_a \hat{a}^\dagger \hat{a} + \hbar\Delta_b \hat{b}^\dagger \hat{b} + \hbar J (\hat{a}^\dagger \hat{b} + \hat{b}^\dagger \hat{a}) + \hbar g \hat{a}^\dagger \hat{a} \hat{q} + \frac{\hat{p}^2}{2m} + \frac{1}{2} m \omega_m^2 \hat{q}^2 + \frac{1}{3} \alpha \hat{q}^3 + i\hbar\epsilon_c (\hat{a}^\dagger - \hat{a}) + i\hbar\epsilon_p (\hat{a}^\dagger e^{-i\delta t} - \hat{a} e^{i\delta t}) \quad (2)$$

in the frame rotating at the frequency of control field ω_c . Here, $\Delta_a = \omega_a - \omega_c$ ($\Delta_b = \omega_b - \omega_c$) is the detuning between the photon mode in cavity a (cavity b) and the control field, while $\delta = \omega_p - \omega_c$ is the detuning between the probe field and the control field. The Heisenberg–Langevin equations of the proposed optomechanical system are then given by

$$\begin{aligned} \frac{d}{dt} \hat{q} &= \frac{\hat{p}}{m}, \\ \frac{d}{dt} \hat{p} &= -m\omega_m^2 \hat{q} - \alpha \hat{q}^2 - \hbar g \hat{a}^\dagger \hat{a} - \gamma_m \hat{p} + \hat{F}_{th}, \\ \frac{d}{dt} \hat{a} &= -[\kappa_a + i(\Delta_a + g\hat{q})] \hat{a} - iJ \hat{b} + \epsilon_c + \epsilon_p e^{-i\delta t} + \hat{a}_{in}, \\ \frac{d}{dt} \hat{b} &= -(\kappa_b + i\Delta_b) \hat{b} - iJ \hat{a} + \hat{b}_{in}. \end{aligned} \quad (3)$$

Here, \hat{F}_{th} is the thermal noise of the mechanical oscillator, and has the relationship of $\langle \hat{F}_{th}(t) \rangle = 0$ and $\langle \hat{F}_{th}(t) \hat{F}_{th}^\dagger(t') \rangle = \gamma_m \int e^{-i\omega(t-t')} \left[\coth\left(\frac{\hbar\omega}{2k_B T}\right) + 1 \right] \frac{d\omega}{2\pi\omega_m}$. k_B and T are the Boltzmann constant and the ambient temperature of the cavity optomechanical system. \hat{a}_{in} and \hat{b}_{in} are the quantum noises of the cavities a and b , respectively, which satisfy the relations: $\langle \hat{a}_{in}(t) \rangle = 0$, $\langle \hat{b}_{in}(t) \rangle = 0$, $\langle \hat{a}_{in}(t) \hat{a}_{in}^\dagger(t') \rangle = \delta(t - t')$, and $\langle \hat{b}_{in}(t) \hat{b}_{in}^\dagger(t') \rangle = \delta(t - t')$. In this work, we are interested in the mean response of the proposed cavity optomechanical system to the probe field. Therefore, the operators \hat{q} , \hat{p} , \hat{a} , and \hat{b} are then reduced to their expectation values, i.e., $q(t) \equiv \langle \hat{q}(t) \rangle$, $p(t) \equiv \langle \hat{p}(t) \rangle$, $a(t) \equiv \langle \hat{a}(t) \rangle$, and $b(t) \equiv \langle \hat{b}(t) \rangle$. In addition, the thermal noise \hat{F}_{th} and quantum noises \hat{a}_{in} and \hat{b}_{in} can be ignored in the following. In this case, the Heisenberg–Langevin equations (3) can be rewritten as the mean value equations

$$\begin{aligned} \frac{d}{dt} q &= \frac{p}{m}, \\ \frac{d}{dt} p &= -m\omega_m^2 q - \alpha q^2 - \hbar g a^\dagger a - \gamma_m p, \\ \frac{d}{dt} a &= -[\kappa_a + i(\Delta_a + gq)] a - iJ b + \epsilon_c + \epsilon_p e^{-i\delta t}, \\ \frac{d}{dt} b &= -(\kappa_b + i\Delta_b) b - iJ a, \end{aligned} \quad (4)$$

where the thermal noise and quantum noise terms are dropped due to the zero mean values of \hat{a}_{in} , \hat{b}_{in} , and \hat{F}_{th} . In addition, the factorization approximation (e.g., $\langle qa \rangle = \langle q \rangle \langle a \rangle$) is used.

It is noted that the driving field is much stronger than the probe field, and thus the solutions of Equation (4) can be written as

$$O = O_s + O_{1+} e^{-i\delta t} + O_{1-} e^{i\delta t} + O_{2+} e^{-2i\delta t} + O_{2-} e^{2i\delta t} \quad (5)$$

with $O = q, p, a, b$. Here, only the first-order and second-order sidebands are considered, while higher-order sidebands are ignored in this work. The term O_s is the steady-state solution of the operator O , the terms $O_{1+} e^{-i\delta t}$ and $O_{1-} e^{i\delta t}$ denote the first-order upper and lower sidebands with the frequencies of ω_p and $2\omega_c - \omega_p$, respectively. The terms

$O_{2+}e^{-2i\delta t}$ and $O_{2-}e^{2i\delta t}$ represent the second-order upper and lower sidebands with the frequencies of $2\omega_p - \omega_c$ and $3\omega_c - 2\omega_p$, respectively.

By substituting Equation (5) into Equation (4), and ignoring the higher-order nonlinear terms, the steady-state solutions O_s provided by the driving field can be obtained as

$$\begin{aligned} p_s &= 0, \\ q_s &= -\frac{\hbar g |a_s|^2}{m\omega_m^2 + \alpha q_s}, \\ a_s &= \frac{\varepsilon_c}{\kappa_a + i\Delta'_a + \frac{J^2}{\kappa_b + i\Delta_b}}, \\ b_s &= \frac{-iJa_s}{\kappa_b + i\Delta_b}, \end{aligned} \tag{6}$$

where $\Delta'_a = \Delta_a + gq_s$ is the effective detuning between the cavity a and the control field. The results of the first-order sideband are given as

$$\begin{aligned} q_{1+} &= \frac{-\hbar g (a_s^* a_{1+} + a_{1-}^* a_s)}{f(\delta)}, \\ q_{1-} &= \frac{-\hbar g (a_s^* a_{1-} + a_{1+}^* a_s)}{f^*(\delta)}, \\ a_{1+} &= \frac{\varepsilon_p [\kappa_a - i(\Delta'_a + \delta) + B(\delta) + i\hbar g^2 |a_s|^2 / f(\delta)]}{d(\delta)}, \\ a_{1-} &= \frac{i\hbar g^2 a_s^2 \varepsilon_p}{d^*(\delta)}, \\ b_{1+} &= \frac{-iJa_{1+}}{\kappa_b + i(\Delta_b - \delta)}, \\ b_{1-} &= \frac{-iJa_{1-}}{\kappa_b + i(\Delta_b + \delta)}. \end{aligned} \tag{7}$$

Here,

$$f(\delta) = m\omega_m^2 + 2\alpha q_s - i\delta m(\gamma_m - i\delta), \tag{8}$$

$$d(\delta) = C(\delta)D(\delta) + i\hbar g^2 |a_s|^2 [C(\delta) - D(\delta)] / f(\delta), \tag{9}$$

and

$$\begin{aligned} A(\delta) &= \frac{J^2}{[\kappa_b + i(\Delta_b - \delta)]}, \\ B(\delta) &= \frac{J^2}{[\kappa_b - i(\Delta_b + \delta)]}, \\ C(\delta) &= \kappa_a + i(\Delta'_a - \delta) + A(\delta), \\ D(\delta) &= \kappa_a - i(\Delta'_a + \delta) + B(\delta). \end{aligned} \tag{10}$$

The coefficient of the second-order upper sideband can also be obtained, which is given as

$$\begin{aligned} a_{2+} &= -\frac{\hbar g^3 a_s^2 q_{1+} a_{1-}^*}{f(2\delta)d(2\delta)} + \frac{iga_s(\hbar ga_{1+} a_{1-}^* + \alpha q_{1+}^2)D(2\delta)}{f(2\delta)d(2\delta)} \\ &\quad - \frac{igq_{1+} a_{1+} [D(2\delta) + i\hbar g^2 |a_s|^2 / f(2\delta)]}{d(2\delta)}. \end{aligned} \tag{11}$$

It can be seen from Equation (11) that the generation of the second-order upper sideband is closely related to the first-order upper sideband (i.e., a_{1+}) and the first-order lower sideband (i.e., a_{1-}) generation.

The output field can be obtained according to the input–output relation [19], which is given as

$$\begin{aligned} \varepsilon_{\text{out}} = & (\varepsilon_c - \sqrt{2\kappa_a}a_s)e^{-i\omega_c t} + (\varepsilon_p - \sqrt{2\kappa_a}a_{1+})e^{-i\omega_p t} \\ & - \sqrt{2\kappa_a}a_{1-}e^{-i(2\omega_c - \omega_p)t} - \sqrt{2\kappa_a}a_{2+}e^{-i(2\omega_p - \omega_c)t} \\ & - \sqrt{2\kappa_a}a_{2-}e^{-i(3\omega_c - 2\omega_p)t}. \end{aligned} \quad (12)$$

Here, the terms $(\varepsilon_c - \sqrt{2\kappa_a}a_s)e^{-i\omega_c t}$ and $(\varepsilon_p - \sqrt{2\kappa_a}a_{1+})e^{-i\omega_p t}$ denote the output fields with the driving frequency ω_c and probe frequency ω_p , respectively. The transmission of the probe field can then be obtained as $t_p = 1 - \sqrt{2\kappa_a}a_{1+}/\varepsilon_p$. The term $-\sqrt{2\kappa_a}a_{1-}e^{-i(2\omega_c - \omega_p)t}$ represents the Stokes field with the frequency of $2\omega_c - \omega_p$. The term $-\sqrt{2\kappa_a}a_{2+}e^{-i(2\omega_p - \omega_c)t}$ describes the output field with the frequency of $\omega_c + 2\delta$, which is related to the second-order upper sideband. In contrast, the second-order lower sideband is denoted by the term $-\sqrt{2\kappa_a}a_{2-}e^{-i(3\omega_c - 2\omega_p)t}$ with the frequency of $\omega_c - 2\delta$. The efficiency of the second-order upper sideband is defined as

$$\eta = \left| \frac{-\sqrt{2\kappa_a}a_{2+}}{\varepsilon_p} \right|. \quad (13)$$

In addition, the associated group delay of the second-order upper sideband is given as [35]

$$\tau = \frac{\partial[\arg(\eta)]}{2\partial\delta}. \quad (14)$$

The positive group delay ($\tau > 0$) indicates the effect of slow light, while the negative group delay ($\tau < 0$) represents the fast light in the second-order upper sideband.

3. Results and Discussion

The parameters involved in this work were adopted from the experimental work that investigated the deceleration, switching, and propulsion of microwave signals in an optomechanical system [23]. Here, the effective mass of the movable mirror is $m = 7$ pg. The mechanical frequency and mechanical damping rate are $\omega_m = 2\pi \times 1.45$ MHz and $\gamma_m = 2\pi \times 9$ Hz, respectively. The optomechanical coupling strength is $g = 2\pi \times 1.26\sqrt{\hbar/(2m\omega_m)}$ Hz/m. The coupling strength J between the two cavities is $J = 2\pi \times 12.5$ kHz. The decay rates of the cavities are $\kappa_a = \kappa_b = 0.1\omega_m$. The frequency of the coupling field is $\omega_c = 2\pi \times 6.07$ GHz. The cavity a is assumed to be driven at the red-detuned mechanical sideband, resulting in the effective detuning $\Delta'_a \approx \omega_m$

The term $\alpha\hat{q}^3/3$ in the Hamiltonian (1) describes the cubic potential energy, which is linearly determined by the nonlinearity strength α . Therefore, the ratio of the cubic potential energy to the quadratic potential energy $r = |(\alpha\hat{q}_0^3/3)/(m\omega_m^2\hat{q}_0^2/2)|$ increases with the nonlinearity strength α . When the nonlinearity strength is $\alpha = 10^8$ N/m², the ratio r is about 0.14. This indicates that the steady-state quadratic potential energy is much larger than the cubic potential energy, and thus, the cubic potential energy can be described as a perturbation.

The efficiency of the second-order upper sideband η as a function of the normalized detuning δ/ω_m with different mechanical nonlinearity strength α is shown in Figure 2. It is found that a sideband dip between two asymmetric sideband peaks appears around the normalized detuning $\delta/\omega_m = 1$. Such a phenomenon can be attributed to the nonlinearity of the proposed coupled optomechanical cavity system with a cubic nonlinear harmonic oscillator, which is quite different from the linear optomechanical cavity system [33,35]. For a conventional cavity optomechanical system with a harmonic mechanical oscillator, a symmetrical transparent window (i.e., OMIT) can be observed under the resonance condition of $\delta = \omega_m$ (i.e., $\omega_c + \omega_m = \omega_p$) [19]. However, the mechanical oscillator with the potential energy of $m\omega_m^2\hat{q}^2/2 + \alpha\hat{q}^3/3$ is not a harmonic oscillator but a cubic nonlinear harmonic oscillator. In this case, this cubic term (i.e., $\alpha\hat{q}^3/3$) changes the frequency of

mechanical oscillator, which is different from the frequency ω_m in the case of harmonic oscillator. Therefore, the system with a cubic nonlinear harmonic oscillator exhibits an asymmetric OMIT window and the transparency peak is also shifted, which has been demonstrated in Refs. [6,48]. It is noted that the second-order sideband originates from the up-conversion of the first-order sideband. This asymmetric OMIT window in the cavity optomechanical system with a cubic mechanical oscillator thus results in an asymmetric spectrum in the efficiency of a second-order sideband. In addition, such phenomenon has also demonstrated in the cavity optomechanical system with a nonlinear Kerr resonator [35].

In the case of $\Delta'_a \approx \omega_m$ and $\delta/\omega_m \approx 1$ shown in Figure 2, the anti-Stokes field is resonantly enhanced, which then results in suppressed second-order sidebands. For the mechanical nonlinearity strength $\alpha = 0 \text{ N/m}^2$, the maximum efficiency is about 0.017%. The maximum efficiency of the second-order upper sideband is then improved to 0.02% when the mechanical nonlinearity strength is $\alpha = 10 \times 10^7 \text{ N/m}^2$. The enhancement in second-order sideband efficiency can be attributed to the nonlinearity of the mechanical oscillator, which improves the four-wave mixing process in the optical cavity [6].

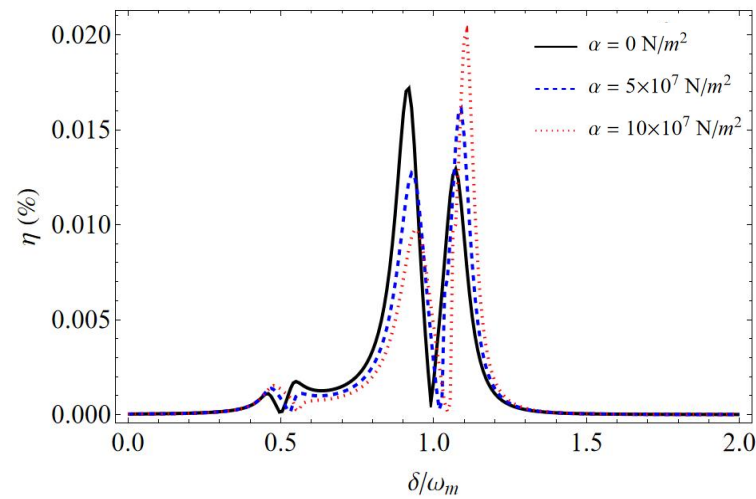


Figure 2. The efficiency η as a function of the normalized detuning δ/ω_m with a different mechanical nonlinearity strength α .

The effects of decay rates κ_a and κ_b on the efficiency of the second-order upper sideband η are shown in Figure 3. Here, the mechanical nonlinearity strength α is fixed at $5 \times 10^7 \text{ N/m}^2$. Figure 3a shows the efficiency η as a function of the normalized detuning δ/ω_m with different decay rates κ_a of cavity a . It is found that the dip of efficiency η is almost unchanged with the variations of κ_a . The values of two asymmetric sideband peaks decreases with the increasing decay rate κ_a of cavity a . For example, the maximum values of efficiency η is 0.016% with $\kappa_a = 0.1\omega_m$, which is about 1.8-fold higher than that with $\kappa_a = 0.2\omega_m$. Therefore, the efficiency of the second-order upper sideband η can be increased by reducing the decay rate κ_a of cavity a . Specifically, the maximum efficiency can be improved to 0.16% with $\kappa_a = 0.01\omega_m$, which is about 10 times that with $\kappa_a = 0.1\omega_m$, and 17.7 times that with $\kappa_a = 0.2\omega_m$. In contrast, the variations in the decay rate κ_b of cavity b do not affect the efficiency of the second-order upper sideband η , as shown in Figure 3b.

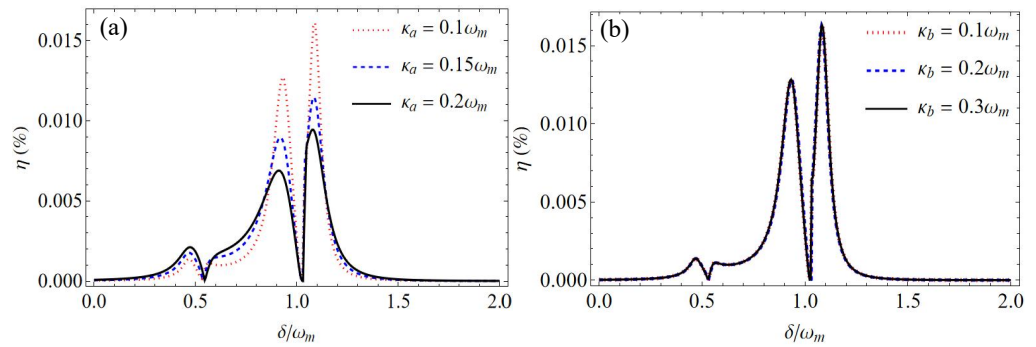


Figure 3. The efficiency η as a function of the normalized detuning δ/ω_m with different cavity decay rates (a) κ_a : $0.1 \omega_m$ (red dotted line), $0.15 \omega_m$ (blue dashed line), and $0.2 \omega_m$ (black solid line) for $\kappa_b = 0.1 \omega_m$, and (b) κ_b : $0.1 \omega_m$ (red dotted line), $0.15 \omega_m$ (blue dashed line), and $0.2 \omega_m$ (black solid line) for $\kappa_a = 0.1 \omega_m$. Here, the mechanical nonlinearity strength is $\alpha = 5 \times 10^7 \text{ N/m}^2$.

The effect of the coupling strength J on the efficiency of the second-order upper sideband η is also discussed. The efficiency η as a function of the normalized detuning δ/ω_m with different coupling strengths J is shown in Figure 4. Here, the mechanical nonlinearity strength is $\alpha = 5 \times 10^7 \text{ N/m}^2$, and the decay rates of cavity a and cavity b are $\kappa_a = \kappa_b = 0.1 \omega_m$. It can be observed from Figure 4 that the dip of efficiency η is not affected by the variations in the coupling strength J . The maximum value of efficiency η decreases with the increase in the coupling strength J . For example, the maximum efficiency of the second-order upper sideband is 0.016% with the coupling strength $J = 2\pi \times 12.5 \text{ kHz}$, while it is decreased to 0.01% with $J = 15\pi \times 12.5 \text{ kHz}$.

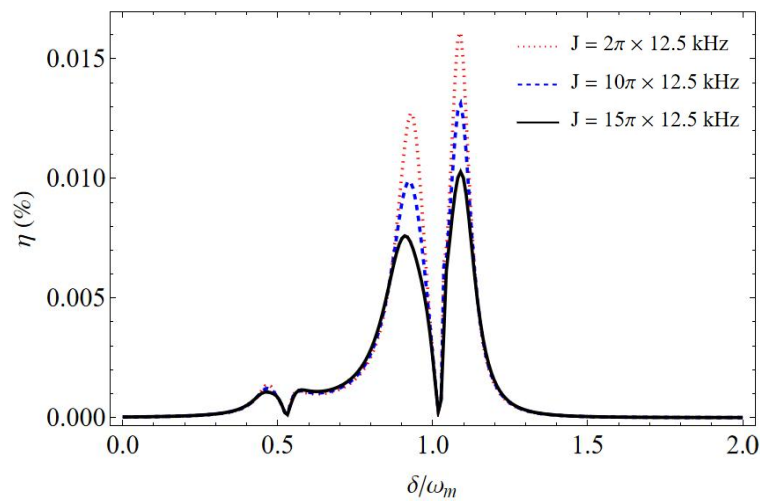


Figure 4. The efficiency η as a function of the normalized detuning δ/ω_m with different coupling strengths J . Here, $\alpha = 5 \times 10^7 \text{ N/m}^2$, and $\kappa_a = \kappa_b = 0.1 \omega_m$.

It should be noted that the mechanical nonlinearity strength α , the cavity decay rates κ_a and κ_b , and the coupling strength J are difficult to tune for a fabricated optomechanical system. However, the optomechanical response of the proposed optomechanical system can be adjusted with the power of the control field and probe field. Figure 5a shows the efficiency of the second-order upper sideband η as a function of the normalized detuning δ/ω_m with the power of the probe field φ_p . Here, the mechanical nonlinearity strength is $\alpha = 10 \times 10^7 \text{ N/m}^2$, cavity decay rates are $\kappa_a = \kappa_b = 0.1 \omega_m$, the coupling strength is $J = 2\pi \times 12.5 \text{ kHz}$, and the power of the control field is fixed at $\varphi_c = 0.02 \mu\text{W}$. It is found that the maximum efficiency increases with the increase in the power of the probe field φ_p . Specifically, the maximum value of η is 0.02% with $\varphi_p = 0.02 \mu\text{W}$, while it is improved to 0.035% with the power of the probe field $\varphi_p = 0.06 \mu\text{W}$. Therefore, the efficiency of the

second-order upper sideband η can be effectively improved by increasing the power of the probe field. For example, the maximum efficiency of 0.203% is achieved with the power of the probe field $\varphi_p = 2 \mu\text{W}$, which is about 10.2 times higher than that with $\varphi_p = 0.02 \mu\text{W}$. The effect of the power of the control field φ_c on the efficiency of the second-order upper sideband η with a fixed power of the probe field φ_p is shown in Figure 5b. It is found that the positions of the efficiency peaks are changed with the variations of φ_c . In addition, compared to the adjustment of the power of the control field φ_c , the variation in the power of the probe field φ_p has less of an impact on the maximum efficiency of the second-order upper sideband.

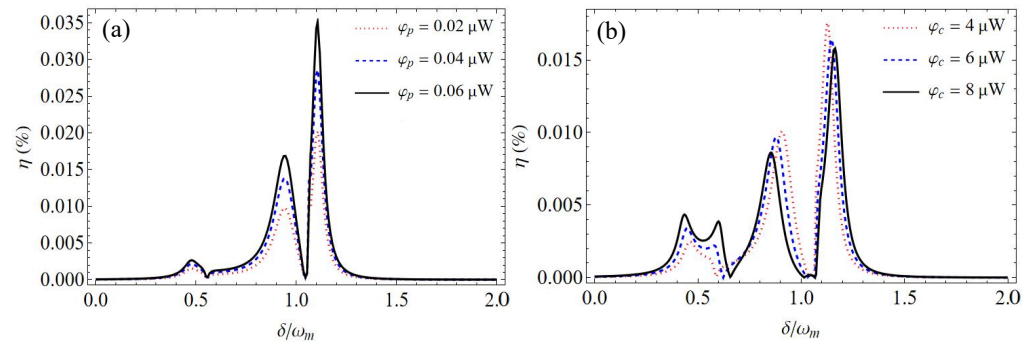


Figure 5. The efficiency η as a function of the normalized detuning δ/ω_m with a different (a) power of the probe field φ_p and (b) power of the control field φ_c . The power of the control field is $\varphi_c = 2 \mu\text{W}$ in (a), and the power of the probe field is $\varphi_p = 0.02 \mu\text{W}$ in (b). Here, the mechanical nonlinearity strength is $\alpha = 10 \times 10^7 \text{ N/m}^2$, cavity decay rates are $\kappa_a = \kappa_b = 0.1 \omega_m$, and the coupling strength is $J = 2\pi \times 12.5 \text{ kHz}$.

The group delays in the proposed coupled optomechanical cavity system with a cubic nonlinear harmonic oscillator were also investigated. The group delay of the transmitted light in a conventional optomechanical system is only related to the power of the control field [20]. Therefore, the effect of the power of control field φ_c on the group delay τ is considered in this work. The group delay τ as a function of the coupling field power φ_c at the resonance $\delta/\omega_m = 1$ with different cavity decay rates κ_a is shown in Figure 6. It was found that only the positive group delay ($\tau > 0$) is observed, which indicates that the slow light effect is achieved with the proposed optomechanical system. For example, the maximum group delay of about 1250 μs is obtained with the power of the control field $\varphi_c = 3.57 \mu\text{W}$ when the decay rate of cavity a is $\kappa_a = 0.1\omega_m$. In addition, the peak position and peak value of the group delay τ decreases with the cavity decay rate κ_a . Specifically, the maximum group delay decreases from 780 μs to 472 μs when the decay rate κ_a is changed from $0.2\omega_m$ to $0.3\omega_m$, and accordingly, the corresponding power of the control field φ_c is changed from 1.87 μW to 1.27 μW . It is worth noting that the positive group delay can also be significantly enhanced with the introduction of cavity b in the coupled optomechanical cavity system. For example, the maximum positive group delay is about 0.007 μs with $\kappa_a = 0.1\omega_m$ in the coupled optomechanical cavity system without cavity b , which is much smaller than that obtained with both cavity a and cavity b (i.e., 1250 μs).

The introduced strong cubic mechanical nonlinearity in the proposed optomechanical system can be obtained with the method proposed in ref. [44]. By coupling the resonators with a low-dimensional auxiliary system, the cubic and even quartic nonlinearity of the mechanical oscillator can be obtained. To obtain a nonlinear harmonic oscillator, a linear mechanical oscillator is coupled to a three-level (qutrit) auxiliary via the interaction μxV . μ is the interaction strength, and V is an operator of the qutrit. x is the dimensionless position of the mechanical oscillator, which has the relationship of $q = \sqrt{\hbar/(m\omega_m)}x$ with the displacement operator q . This qutrit has a diagonal auxiliary Hamiltonian \tilde{H}_0 that is evenly separated by Δ , and its energy levels are $E_n^{(0)} = n\Delta$ ($n = 0, 1, 2$). By placing the auxiliary qutrit in the eigenstate with the energy level E_1 and choosing an appropriate

operator V , a cubic potential term in the form of $2\hbar\Delta(\mu/\Delta)^3x^3$ can be achieved with the mechanical oscillator. If the interaction strength μ is $2\pi \times 3.7$ MHz, and Δ is $2\pi \times 5$ GHz, the mechanical nonlinearity strength α of 1.2×10^8 N/m² can be obtained [6], which is quite close to the value of α used in this work. Such an approach to obtaining a cubic nonlinear harmonic oscillator was also adopted in Refs. [6,50].

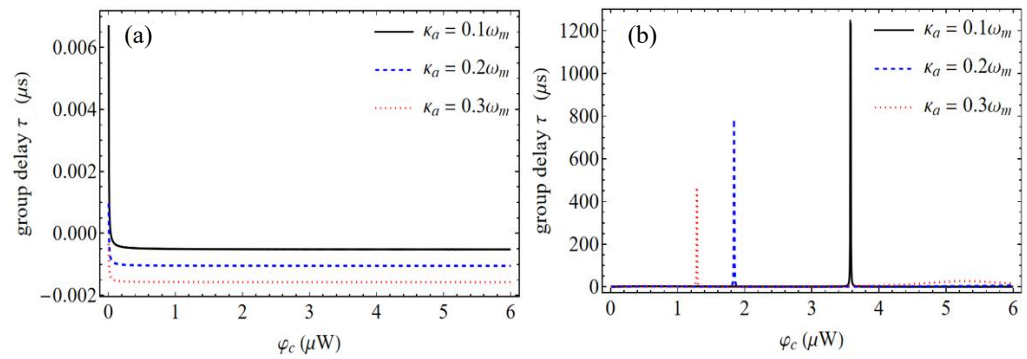


Figure 6. Group delay τ as a function of the coupling field power φ_c at the resonance $\delta/pomega_{a_m} = 1$ with different cavity decay rates κ_a for the proposed coupled optomechanical cavity system with (a) both the cavity a and cavity b, and (b) only cavity a. Here, $\kappa_b = 0.1 \omega_m$, and the mechanical nonlinearity strength is $\alpha = 5 \times 10^7$ N/m².

4. Conclusions

In summary, the generation of second-order sidebands and group delays in a coupled optomechanical cavity system with a cubic nonlinear harmonic oscillator is investigated. The influence of the mechanical nonlinearity strength, the cavity decay rate, the coupling strength between two cavities, the power of the control field, and the power of the probe field on the efficiency of the second-order upper sideband are studied. It is found that the efficiency can be effectively enhanced by reducing the decay rate of cavity a , increasing the coupling strength J and the power of the probe field φ_p . The enhanced generation efficiency of second-order sidebands is helpful in frequency conversion for all-optical network communication. In addition, the slow light effect can be achieved with the proposed optomechanical system. The maximum value of the group delay can be effectively controlled by the power of the control field and the decay rate of cavity a .

Author Contributions: Conceptualization, Q.Z. and Y.X.; methodology, Q.Z. and Y.X.; investigation, Q.Z., Y.H. and Y.X.; writing—original draft preparation, Q.Z.; writing—review and editing, Q.Z., Y.H., Y.Y., H.Z. and Y.X.; supervision, Y.H.; project administration, Y.H. All authors have read and agreed to the published version of the manuscript.

Funding: This research was funded by the National Natural Science Foundation of China (Grant No. 12174243).

Institutional Review Board Statement: Not applicable.

Informed Consent Statement: Not applicable.

Data Availability Statement: Data underlying the results presented in this paper are not publicly available at this time, but may be obtained from the authors upon reasonable request.

Conflicts of Interest: The authors declare no conflicts of interest.

References

1. Aspelmeyer, M.; Kippenberg, T.J.; Marquardt, F. Cavity optomechanics. *Rev. Mod. Phys.* **2014**, *86*, 1391. [CrossRef]
2. Stannigel, K.; Rabl, P.; Sørensen, A.S.; Zoller, P.; Lukin, M.D. Opto-mechanical transducers for long-distance quantum communication. *Phys. Rev. Lett.* **2010**, *105*, 220501. [CrossRef]
3. Gavartin, E.; Verlot, P.; Kippenberg, T.J. A hybrid on-chip optomechanical transducer for ultra-sensitive force measurements. *Nat. Nanotechnol.* **2012**, *7*, 509–514. [CrossRef]

4. Clark, J.B.; Lecocq, F.; Simmonds, R.W.; Aumentado, J.; Teufel, J.D. Sideband cooling beyond the quantum backaction limit with squeezed light. *Nature* **2017**, *541*, 191–195. [[CrossRef](#)]
5. Qiu, L.; Shomroni, I.; Seidler, P.; Kippenberg, T.J. Laser cooling of a nanomechanical oscillator to its zero-point energy. *Phys. Rev. Lett.* **2020**, *124*, 173601. [[CrossRef](#)]
6. Huang, S.; Hao, H.; Chen, A. The optomechanical response of a cubic anharmonic oscillator. *Appl. Sci.* **2020**, *10*, 5719. [[CrossRef](#)]
7. Lemonde, M.A.; Didier, N.; Clerk, A.A. Nonlinear interaction effects in a strongly driven optomechanical cavity. *Phys. Rev. Lett.* **2013**, *111*, 053602. [[PubMed](#)]
8. Børkje, K.; Nunnenkamp, A.; Teufel, J.D.; Girvin, S.M. Signatures of nonlinear cavity optomechanics in the weak coupling regime. *Phys. Rev. Lett.* **2013**, *111*, 053603. [[CrossRef](#)] [[PubMed](#)]
9. Riedinger, R.; Hong, S.; Norte, R.A.; Slater, J.A.; Shang, J.; Krause, A.G.; Anant, V.; Aspelmeyer, M.; Groblacher, S. Non-classical correlations between single photons and phonons from a mechanical oscillator. *Nature* **2016**, *530*, 313–316. [[CrossRef](#)] [[PubMed](#)]
10. Paternostro, M.; Vitali, D.; Gigan, S.; Kim, M.S.; Brukner, C.; Eisert, J.; Aspelmeyer, M. Creating and probing multipartite macroscopic entanglement with light. *Phys. Rev. Lett.* **2007**, *99*, 250401. [[CrossRef](#)] [[PubMed](#)]
11. Palomaki, T.A.; Teufel, J.D.; Simmonds, R.W.; Lehnert, K.W. Entangling mechanical motion with microwave fields. *Science* **2013**, *342*, 710–713. [[CrossRef](#)] [[PubMed](#)]
12. Grblacher, S.; Hammerer, K.; Vanner, M.R.; Aspelmeyer, M. Observation of strong coupling between a micromechanical resonator and an optical cavity field. *Nature* **2009**, *460*, 724–727. [[CrossRef](#)]
13. Dobrindt, J.M.; Wilson-Rae, I.; Kippenberg, T.J. Parametric Normal-mode splitting in cavity optomechanics. *Phys. Rev. Lett.* **2008**, *101*, 263602. [[CrossRef](#)] [[PubMed](#)]
14. Rossi, M.; Kralj, N.; Zippilli, S.; Natali, R.; Borrielli, A.; Pandraud, G.; Serra, E.; Di Giuseppe, G.; Vitali, D. Normal-mode splitting in a weakly coupled optomechanical system. *Phys. Rev. Lett.* **2018**, *120*, 073601. [[CrossRef](#)]
15. Jaehne, K.; Genes, C.; Hammerer, K.; Wallquist, M.; Polzik, E.S.; Zoller, P. Cavity-assisted squeezing of a mechanical oscillator. *Phys. Rev. A* **2009**, *79*, 063819. [[CrossRef](#)]
16. Agarwal, G.S.; Huang, S. Strong mechanical squeezing and its detection. *Phys. Rev. A* **2016**, *93*, 043844. [[CrossRef](#)]
17. Wollman, E.E.; Lei, C.U.; Weinstein, A.J.; Suh, J.; Kronwald, A.; Marquardt, F.; Clerk, A.A.; Schwab, K.C. Quantum squeezing of motion in a mechanical resonator. *Science* **2015**, *349*, 952–955. [[CrossRef](#)]
18. Agarwal, G.S.; Huang, S. Electromagnetically induced transparency in mechanical effects of light. *Phys. Rev. A* **2010**, *81*, 041803. [[CrossRef](#)]
19. Weis, S.; Riviere, R.; Deleglise, S.; Gavartin, E.; Arcizet, O.; Schliesser, A.; Kippenberg, T.J. Optomechanically induced transparency. *Science* **2010**, *330*, 1520–1523. [[CrossRef](#)]
20. Safavi-Naeini, A.H.; Alegre, T.M.; Chan, J.; Eichenfield, M.; Winger, M.; Lin, Q.; Hill, J.T.; Chang, D.E.; Painter, O. Electromagnetically induced transparency and slow light with optomechanics. *Nature* **2011**, *472*, 69–73. [[CrossRef](#)]
21. Dong, C.; Fiore, V.; Kuzyk, M.C.; Wang, H. Transient optomechanically induced transparency in a silica microsphere. *Phys. Rev. A* **2013**, *87*, 055802. [[CrossRef](#)]
22. Jain, M.; Xia, H.; Yin, G.Y.; Merriam, A.J.; Harris, S.E. Efficient nonlinear frequency conversion with maximal atomic coherence. *Phys. Rev. Lett.* **1996**, *77*, 4326. [[CrossRef](#)] [[PubMed](#)]
23. Zhou, X.; Hocke, F.; Schliesser, A.; Marx, A.; Huebl, H.; Gross, R.; Kippenberg, T.J. Slowing, advancing and switching of microwave signals using circuit nanoelectromechanics. *Nat. Phys.* **2013**, *9*, 179–184. [[CrossRef](#)]
24. Lvovsky, A.I.; Sanders, B.C.; Tittel, W. Optical quantum memory. *Nat. Photonics* **2009**, *3*, 706–714. [[CrossRef](#)]
25. Agarwal, G.S.; Huang, S. Optomechanical systems as single photon routers. *Phys. Rev. A* **2012**, *85*, 021801(R). [[CrossRef](#)]
26. Karuza, M.; Biancofiore, C.; Bawaj, M.; Molinelli, C.; Galassi, M.; Natali, R.; Tombesi, P.; Di Giuseppe, G.; Vitali, D. Optomechanically induced transparency in a membrane-in-the-middle setup at room temperature. *Phys. Rev. A* **2013**, *88*, 013804. [[CrossRef](#)]
27. Xiong, H.; Wu, Y. Fundamentals and applications of optomechanically induced transparency. *Appl. Phys. Rev.* **2018**, *5*, 031305. [[CrossRef](#)]
28. Chen, B.; Jiang, C.; Zhu, K.D. Slow light in a cavity optomechanical system with a Bose–Einstein condensate. *Phys. Rev. A* **2011**, *83*, 055803. [[CrossRef](#)]
29. Akram, M.J.; Khan, M.M.; Saif, F. Tunable fast and slow light in a hybrid optomechanical system. *Phys. Rev. A* **2015**, *92*, 023846. [[CrossRef](#)]
30. Lü, H.; Wang, C.; Yang, L.; Jing, H. Optomechanically induced transparency at exceptional points. *Phys. Rev. Appl.* **2018**, *10*, 014006. [[CrossRef](#)]
31. Jiang, C.; Cui, Y.; Zhai, Z.; Yu, H.; Li, X.; Chen, G. Phase-controlled amplification and slow light in a hybrid optomechanical system. *Opt. Express* **2019**, *27*, 30473–30485. [[CrossRef](#)]
32. Xu, Y.; Liu, W. Fano resonance and slow-to-fast light conversion in a Laguerre–Gaussian rovibrational cavity. *J. Lightwave Technol.* **2022**, *41*, 2246–2251. [[CrossRef](#)]
33. Xiong, H.; Si, L.G.; Zheng, A.S.; Yang, X.X.; Wu, Y. Higher-order sidebands in optomechanically induced transparency. *Phys. Rev. A* **2012**, *86*, 013815. [[CrossRef](#)]
34. Kronwald, A.; Marquardt, F. Optomechanically induced transparency in the nonlinear quantum regime. *Phys. Rev. Lett.* **2013**, *111*, 133601. [[CrossRef](#)] [[PubMed](#)]

35. Jiao, Y.F.; Lu, T.X.; Jing, H. Optomechanical second-order sidebands and group delays in a Kerr resonator. *Phys. Rev. A* **2018**, *97*, 013843. [[CrossRef](#)]
36. Wang, B.; Liu, Z.X.; Xiong, H.; Wu, Y. Highly sensitive mass sensing by means of the optomechanical nonlinearity. *IEEE Photonics J.* **2018**, *10*, 6803908. [[CrossRef](#)]
37. Kong, C.; Xiong, H.; Wu, Y. Coulomb-interaction-dependent effect of high-order sideband generation in an optomechanical system. *Phys. Rev. A* **2017**, *95*, 033820. [[CrossRef](#)]
38. Xiong, H.; Si, L.G.; Wu, Y. Precision measurement of electrical charges in an optomechanical system beyond linearized dynamics. *Appl. Phys. Lett.* **2017**, *110*, 171102. [[CrossRef](#)]
39. Chen, B.; Shang, L.; Wang, X.F.; Chen, J.B.; Xue, H.B.; Liu, X.; Zhang, J. Atom-assisted second-order sideband generation in an optomechanical system with atom-cavity-resonator coupling. *Phys. Rev. A* **2019**, *99*, 063810. [[CrossRef](#)]
40. Catalini, L.; Rossi, M.; Langman, E.C.; Schliesser, A. Modeling and observation of nonlinear damping in dissipation-diluted nanomechanical resonators. *Phys. Rev. Lett.* **2021**, *126*, 174101. [[CrossRef](#)]
41. Lü, X.Y.; Liao, J.Q.; Tian, L.; Nori, F. Steady-state mechanical squeezing in an optomechanical system via Duffing nonlinearity. *Phys. Rev. A* **2015**, *91*, 013834. [[CrossRef](#)]
42. Huang, P.; Zhou, J.; Zhang, L.; Hou, D.; Lin, S.; Deng, W.; Meng, C.; Duan, C.; Ju, C.; Zheng, X.; et al. Generating giant and tunable nonlinearity in a macroscopic mechanical resonator from a single chemical bond. *Nat. Commun.* **2016**, *7*, 11517. [[CrossRef](#)]
43. Kaajakari, V.; Mattila, T.; Oja, A.; Seppa, H. Nonlinear limits for single-crystal silicon microresonators. *J. Microelectromech. Syst.* **2004**, *13*, 715–724. [[CrossRef](#)]
44. Jacobs, K.; Landahl, A.J. Engineering giant nonlinearities in quantum nanosystems. *Phys. Rev. Lett.* **2009**, *103*, 067201. [[CrossRef](#)] [[PubMed](#)]
45. Grimm, M.; Bruder, C.; Lörch, N. Optomechanical self-oscillations in an anharmonic potential: Engineering a nonclassical steady state. *J. Opt.* **2016**, *18*, 094004. [[CrossRef](#)]
46. Djorwé, P.; Engo, S.N.; Woafu, P. Robustness of continuous-variable entanglement via geometrical nonlinearity. *Phys. Rev. A* **2014**, *90*, 024303. [[CrossRef](#)]
47. Hao, H.; Huang, S.; Chen, A. Normal mode splitting in a cavity optomechanical system with a cubic anharmonic oscillator. *Int. J. Theor. Phys.* **2021**, *60*, 2766–2777. [[CrossRef](#)]
48. Lv, W.; Deng, L.; Huang, S.; Chen, A. Optomechanically induced transparency in optomechanical system with a cubic anharmonic oscillator. *Photonics* **2023**, *10*, 407. [[CrossRef](#)]
49. Saiko, A.P.; Fedaruk, R.; Markevich, S. Kerr-like nonlinearities in an optomechanical system with an asymmetric anharmonic mechanical resonator. *JETP Lett.* **2021**, *113*, 487–492. [[CrossRef](#)]
50. Huang, S.; Wu, Y.; Chen, A. The stationary optomechanical entanglement between an optical cavity field and a cubic anharmonic oscillator. *Int. J. Theor. Phys.* **2021**, *60*, 3961–3972. [[CrossRef](#)]
51. Latmiral, L.; Armata, F.; Genoni, M.G.; Pikovski, I.; Kim, M. Probing anharmonicity of a quantum oscillator in an optomechanical cavity. *Phys. Rev. A* **2016**, *93*, 052306. [[CrossRef](#)]
52. Yaris, R.; Bendler, J.; Lovett, R.A.; Bender, C.M.; Fedders, P.A. Resonance calculations for arbitrary potentials. *Phys. Rev. A* **1978**, *18*, 1816. [[CrossRef](#)]
53. Alvarez, G. Coupling-constant behavior of the resonances of the cubic anharmonic oscillator. *Phys. Rev. A* **1988**, *37*, 4079. [[CrossRef](#)] [[PubMed](#)]
54. Cveticanin, L.; Zukovic, M.; Mester, G.; Biro, I.; Sarosi, J. Oscillators with symmetric and asymmetric quadratic nonlinearity. *Acta Mech.* **2016**, *227*, 1727–1742. [[CrossRef](#)]
55. Bender, C.M.; Dunne, G.V. Large-order perturbation theory for a non-Hermitian PT-symmetric Hamiltonian. *J. Math. Phys.* **1998**, *40*, 4616–4621. [[CrossRef](#)]
56. Bender, C.M.; Weniger, E.J. Numerical evidence that the perturbation expansion for a non-Hermitian PT-symmetric Hamiltonian is Stieltjes. *J. Math. Phys.* **2001**, *42*, 2167–2183. [[CrossRef](#)]
57. Mera, H.; Pedersen, T.G.; Nikolić, B.K. Nonperturbative quantum physics from low-order perturbation theory. *Phys. Rev. Lett.* **2015**, *115*, 143001. [[CrossRef](#)]

Disclaimer/Publisher's Note: The statements, opinions and data contained in all publications are solely those of the individual author(s) and contributor(s) and not of MDPI and/or the editor(s). MDPI and/or the editor(s) disclaim responsibility for any injury to people or property resulting from any ideas, methods, instructions or products referred to in the content.